JOURNAL OF MATERIALS SCIENCE 33 (1998) 3085–3093

Polymer matrix composites: Conductivity enhancement through polypyrrole coating of nickel flake

W. B. GENETTI, W. L. YUAN, B. P. GRADY, E. A. O'REAR, C. L. LAI
School of Chemical Engineering and Materials Science, The University of Oklahoma, Norman, OK 73019, USA

D. T. GLATZHOFER
Department of Chemistry and Biochemistry, The University of Oklahoma, Norman, OK 73019, USA
E-mail: bpgrady@mathost.ecn.au.edu

The electrical resistance of polymeric materials loaded with conductive fillers can be divided into three major categories: the intrinsic resistance of the filler and matrix, the particle–particle contact resistance, and the tunnelling resistance. A method for decreasing both the particle–particle contact and the tunnelling resistance in nickel-filled low-density polyethylene composites which involves coating the nickel with polypyrrole (PPy) using admicellar polymerization has been developed. It is believed that these resistances are reduced by the formation of PPy ''molecular wires'' which occur as a result of chain entanglements at high filler loadings. Coating the nickel particles with PPy leads to a three-order-of-magnitude increase in conductivity at concentrations well above the percolation threshold without significantly changing the thermal or mechanical properties of the composite.

1. Introduction

Electrically conducting thermoplastic composites are a class of materials that consist of a conductive filler supported by an insulating polymer matrix. These composites have several advantages over other conductive materials including processability, flexibility, ability to absorb mechanical shock, light weight, corrosion resistance, ability to form complex parts, parts consolidation and conductivity control [1]. Research in conductive composites was initiated to find a lightweight inexpensive method for electromagnetic shielding of computers and electronic equipment as these devices moved from shielded rooms to desktops in homes and offices. Examples of other applications, both present and future, include conductive adhesives, underfill for flip chips, cold solders, switching devices, static charge-dissipating materials, and devices for surge protection [2].

The easiest method of producing conductive composites is to fill an insulating polymer having good mechanical properties with highly conductive particles, such as metal powders or carbon black. Two landmark studies of conduction in metal filled polymers were reported by Gurland [3] in 1966 and Malliaris and Turner [4] in 1971. Gurland studied hot-pressed polymers filled with sintered silver–alumina and showed that there was a relationship between the degree of contiguity or connectedness and conduction [3]. In order to achieve conduction in filled polymer systems, conductive pathways of filler particles are required throughout the polymer matrix so as to allow electrons to move freely through the material. Percolation theory quantitatively relates the electrical conductivity of the composite to the volume fraction of the filler [5]. The critical volume fraction, V_c, also called the percolation threshold, is the lowest concentration of filler that forms continuous conductive pathways throughout the polymer matrix. The composite conductivity increases slowly with increasing filler concentration until the critical volume fraction is reached [6]. At V_c a very sharp jump in conductivity is obtained over a very small concentration range, referred to as the critical region. In the critical region the conductivity, σ, and concentration have a power-law relationship as given by

$$\sigma \propto (V - V_c)^t \quad (1)$$

where V is the volume fraction [7]. The power-law index, t, is a function of the interactions between the polymer and the matrix [8]. The critical region ends when all the filler particles are involved in at least one conductive pathway and higher filler concentrations only achieve moderate changes in conductivity.

The percolation threshold is affected by the size and shape of the filler particles. As the size of the

filler particles decreases, the surface area available for conductive contacts increases relative to particle volume, thus causing the formation of conductive pathways at lower volume fractions. Increasing the aspect ratio (length divided by diameter); increases the average number of contacts per particle and conductive pathways occur at lower volume fractions [9]. V_c is also affected by the dispersion and morphology of the filler particles. Malliaris and Turner [4] studied pressed powder-mixed composites of nickel-filled polyethylene and poly(vinyl chloride) resins which formed segregated phases of metal and polymer. By increasing the degree of segregation, the critical volume fraction was reduced. This segregation can be induced by choosing a semicrystalline polymer as the matrix. Bigg [10] has shown that the filler particles are excluded from the crystalline regions of the sample, thus increasing the absolute filler concentration in the amorphous regions. Since the amorphous regions of the polymer tend to be continuous, conductive pathways form at lower bulk concentrations, thus requiring a lower filler content to achieve the same conductivity.

Above the critical volume fraction, the composite conductivity is affected by the intrinsic conductivity of the filler and matrix, and polymer–filler interactions. In systems with a high polymer–filler adhesion, the polymer forms a thick film around the conductive filler which limits the particle–particle contact; thus the composite has a low conductivity but good mechanical properties. In systems with weak polymer–filler adhesion, the particles have a higher probability of contacting, but the mechanical properties deteriorate significantly [11].

The resistance to electron flow in conductive composites is comprized of three resistances: the intrinsic resistivity of the filler material, the particle–particle contact resistance and the tunnelling resistance [12]. The particle–particle contact resistance is the resistance due to the forcing of an electron through a small area. The tunnelling resistance is a result of electrons passing through a very thin insulating film which is possible when the film thickness is less than 100 Å. Any modifications to the composite which affect at least one of the three resistances can change the composite conductivity.

Because of the importance of the polymer–filler interactions on the physical properties of the polymer matrix composite, modification of the filler surface can lead to changes in the overall properties. Previous studies indicate that the surface of inorganic particulates, such as silica, alumina, titanium dioxide or copper oxide, can be modified by the addition of conductive polymer films inducing changes in the overall conductivity and/or surface morphology [13–15]. Because conductive polymers are intractable, the films are formed by polymerization on the surface of the particulate by techniques such as electrochemical oxidation, chemical initiation or chemically initiated polymerization on surfaces with oxidative sites [16–18]. The addition of ultrathin, electrically conductive polymer films changes the nature of the interaction between the particles, thus effecting the physical properties of the composite.

Others have reported changes in specific mechanical properties of particulate-filled polymer–matrix composites through the modification of the filler surface. For example, methacrylate and epoxy functional silane coupling agents have been used to modify clay, wollastonite and quartz particulates in polyolefin composites [19]. The composites with the coupling agents have higher moduli, stiffnesses and strength-to-weight ratios than composites made from the unmodified fillers. The mechanical strength of polymer–matrix composites with inorganic particulate fillers, such as silica, has also been enhanced by the addition of an ultrathin coating added by admicellar polymerization. The ultrathin polymer film apparently makes the filler more compatible with the polymer host by building a bridge of physical bonds between the filler and the matrix [20]. This study reports the increase in electrical conductivity above the percolation threshold due to the addition of an ultrathin conducting polymer film on the filler surface. To date, we are aware of no prior studies of increasing the conductivity of particulate filled polymer–matrix composites above the percolation threshold.

In this study, the surface of a nickel flake was modified by the addition of polypyrrole (PPy), an intrinsically conductive polymer, by admicellar polymerization. The flakes were characterized by both an optical microscopy and scanning tunnelling microscopy (STM) in order to determine the nature of the coating. Both nickel and the modified nickel were incorporated into a low-density polyethylene (LDPE) matrix and the electrical conductivities of the two samples were measured as functions of concentration. In addition, the fractional crystallinities of the LDPE and tensile properties of the composites were also determined.

Experimental procedure

2.1. Admicellar polymerization

Admicellar polymerization is a method of modifying the surface of an inorganic powder through the addition of an ultrathin polymeric film [21]. A schematic representation of the four-step process, namely, admicelle formation, solubilization, polymerization and washing, is shown in Fig. 1.

2.1.1. Admicelle formation

A bilayer of surfactant, called an admicelle, was adsorbed on the surface of the nickel flake in water. The pH was adjusted to below the point of zero charge (PZC) so that the polar head groups of the anionic surfactant were attracted and held to the substrate surface by electrostatic charge. Assuming the nickel flakes had a thin nickel oxide layer, as has been shown in the literature, the PZC is approximately 8.80 [22]. Nickel flake (50 g, Alfa Aesar), with an average diameter of 44 μm, and thickness of 0.37 μm, was placed in 1 l of 7.5 mM sodium dodecyl sulphate (Sigma) (see Fig. 1) at pH 4.5. This surfactant concentration is below the critical micelle concentration but sufficiently high to favour admicelle formation on the particle surface.

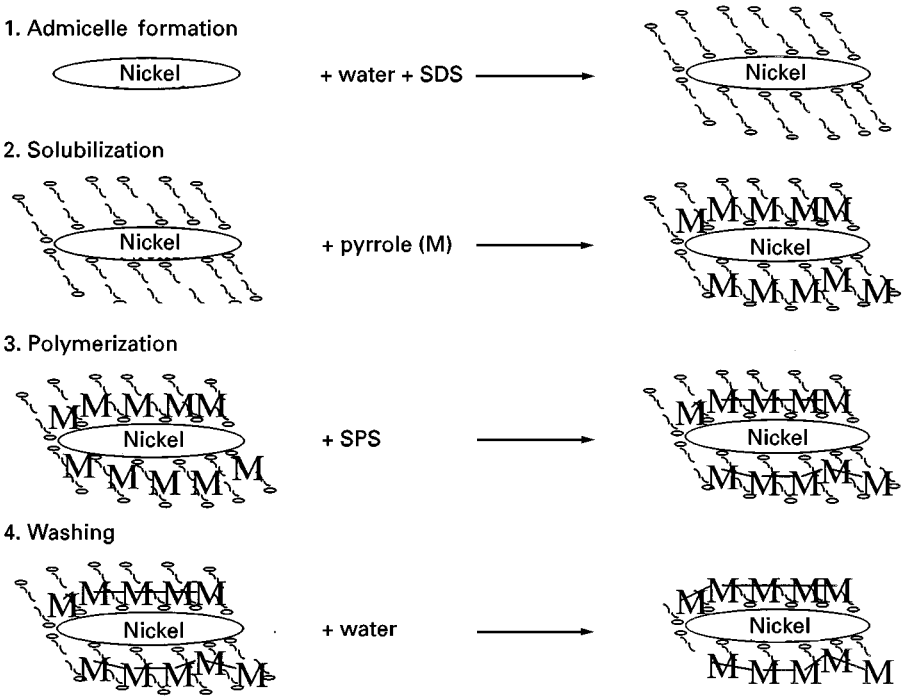

Figure 1 Steps in admicellar polymerization of PPy on a nickel flake surface. SDS, sodium dodecyl sulfate; SPS, sodium persulfate.

The above solution was mixed for 24 h with mechanical agitation to keep the nickel particles suspended in the mixture.

2.1.2. Solubilization

Pyrrole (Sigma) was purified by passing it through a packed bed of basic alumina (Sigma). 20 mmol of pyrrole was then added to the mixture and the solution was once again allowed to mix for another 24 h to assure that the system had equilibrated. Pyrrole has a relatively low water solubility and preferentially partitions into the admicellar layer.

2.1.3. Polymerization

Oxidative polymerization was used to react the monomer inside the admicelle using a water-soluble "initiator". The initiator, sodium persulfate (20 mmol; Aldrich) (see Fig. 1) was dissolved in a minimal amount of water and added to the reaction vessel at 25 °C. Materials were reacted for 2 h to assure completion.

2.1.4. Washing

After polymerization, the modified nickel was collected by filtration and washed with water. The modified nickel was air dried and then placed in a vacuum oven at 70 °C for 24 h to remove residual water.

2.2. Particulate characterization

2.2.1. Weight fraction of polypyrrole

Samples of both nickel and PPy-coated nickel were placed in a Linburg Hevi-Duty furnace overnight at 800 °C to remove the PPy coating by burning. The samples were weighed in a Mettler H31AR balance before and after burning. Assuming that the nickel oxidations were the same for both samples, the weight fraction of PPy was determined from a mass balance.

2.2.1. Optical microscopy

A Nikon optical microscope at a magnification of 800 × was used to observe the large-scale structure of the particles to determine whether a substantial number of PPy particles were mixed with the modified nickel.

2.2.3. Atomic force microscopy and scanning tunnelling microscopy

Atomic Force Microscopy (AFM) and STM were done using a Multimode NanoScope III SPM (Digital Instruments) microscope. STM was done in both standard height mode and current imaging tunnelling spectroscopy (CITS) mode with mechanically cut Pt–Ir tips. A CITS image is a collection of scanning tunnelling spectroscopy (STS) plots which correspond to a data point in a STM image. A STS curve is a plot of the tunnelling current at a specific surface position obtained as a function of the bias voltage applied to the sample at a fixed separation from the scanning tip. CITS reveals the conductivity distribution in the scanned area. Samples of both the nickel and the PPy-coated nickel were prepared by evenly pressing a small amount of flake on a thick layer of parafilm. A conducting path between the flakes and the bottom steel sample holder was constructed with silver glue. This sandwich structure (flakes–parafilm–steel disc) ensured that the images obtained were only a function of the surface morphology of the flakes.

2.3. Film preparation

LDPE was dissolved in 1.5 ml of xylene (Aldrich) per gram of polymer at 110 °C. LDPE (Aldrich) was a highly branched low-molecular-weight polymer with a density of 0.906 g cm^{-3}. The weight-averaged molecular weight was 35 000 g mol^{-1} and the polydispersity index was 4.5. The melting point of the material was 83 °C and the melt flow index was 2250 g per 10 min. This LDPE was chosen as the matrix because the combination of its properties leads to a polyethylene which is soluble in xylene at high polymer concentrations. Nickel or PPy-coated nickel was added and the mixture was allowed to reheat to 110 °C. After reheating, the mixture was stirred for 2 min and then cast onto a 70 °C mercury surface. LDPE quickly formed a gel which did not allow the filler particles to settle from solution. The composite was left with a covering permeable to the solvent under a chemical hood for 48 h. The composite film was removed from the mercury surface and allowed to dry for another 48 h at 25 °C under the hood. Residual solvent was then removed by placing the sample in a vacuum oven at 70 °C for an additional 48 h. The film thickness was measured using a micrometer and varied from 0.6 to 0.9 mm.

2.4. Conductivity measurements

Depending on the filler loading of the composite, one of two methods was used to measure the direct-current (d.c.) electrical conductivity. The conductivity at high filler loading was measured using a four-point probe geometry, as outlined in the American Standard for Testing and Materials (ASTM) Standard D 4496 for moderately conductive materials. Copper electrodes were attached using a silver conductive epoxy (Tra-con BA-2902). The current was sent through the outer electrodes using a Keithley 610C electrometer as a current source and the voltage was measured using a Keithley 176 multimeter. The resistance, R, of the composite was determined from the linear portion of the current versus voltage curve by linear regression. The resistivity was calculated using

$$\rho = \frac{1}{\sigma} = \frac{Rab}{c} \tag{2}$$

where a is the film thickness, b is the width and c is the length as shown in Fig. 2a.

The conductivity of the composite films with low filler loading was measured using the sandwich method as outlined in ASTM Standard D 257 for insulating materials. The composite film had two copper electrodes attached with a silver conductive epoxy (Tri-Con BA-2902). The current was passed through the electrodes using an Instek model PS-6010 power supply and the voltage drop across the film was measured by a Hewlett–Packard 3460A digital voltmeter. Equation 2 was used to determine the resistivity, but with the dimension parameters a being the height, b the width, and c the distance between electrodes, as shown in Fig. 2b.

Fig. 2c shows the geometry for the conductivity measurements of the flakes used as fillers in this study.

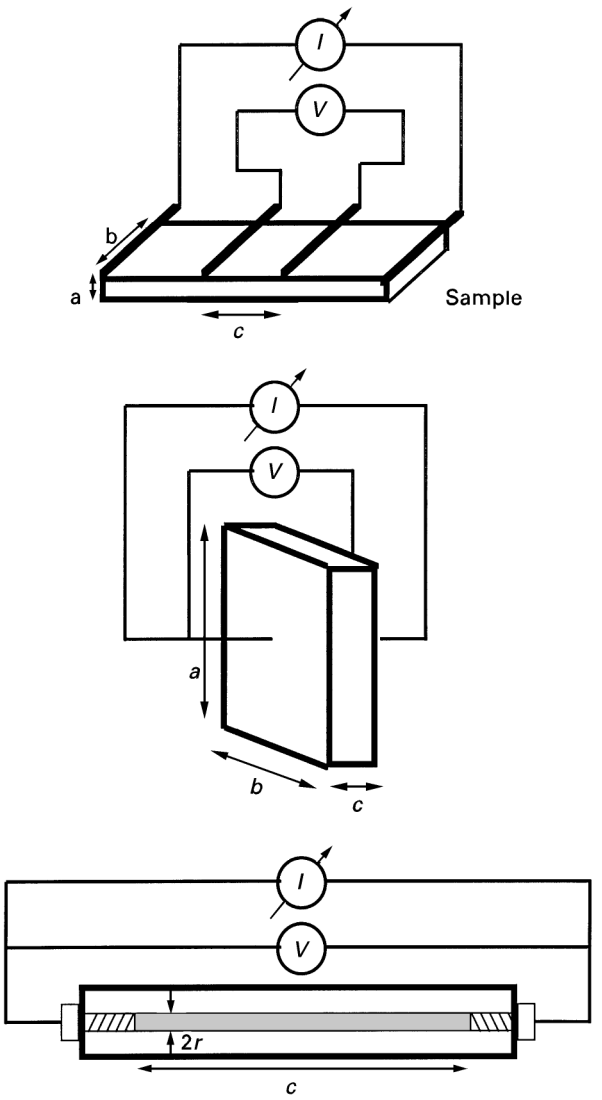

Figure 2 Geometry of conduction measurements: (a) four-point probe of matrix composites; (b) two-point sandwich of matrix composites; (c) powder testing of nickel filler and PPy-coated filler. a, b and c are the sample dimensions, I is the induced current and V is the measured voltage.

Vibrational packing facilitated the maximum possible packing in the sample cell. A current was induced through the sample with an Instek model PS-6010 d.c. power supply and the voltage drop across the sample cell was measured using a Hewlett–Packard 3460A digital voltmeter. The following equation yielded the conductivity of the fillers:

$$\rho = \frac{1}{\sigma} = \frac{R\pi r^2}{c} \tag{3}$$

r being the diameter and c the length of the conductivity chamber as shown in Fig. 2c.

2.5. Crystallinity

The crystallinity was determined by differential scanning calorimetry (DSC) measurements using a Perkin–Elmer DSC II calorimeter at a scanning rate of 20 °C min^{-1} and a computerized data acquisition system designed at the University of Oklahoma. The heat

of melting, ΔH_f, for a sample of known polymer mass and the heat of melting, ΔH_f^0, for a purely crystalline polymer gave the crystallinity, χ, according to [23]

$$\chi = \frac{\Delta H_f}{\Delta H_f^0} \quad (4)$$

The heat of melting for a sample was determined experimentally by integrating the baseline subtracted DSC output over the temperature range in which the sample melts [24]. The literature value of the heat of melting for pure crystalline LDPE was 282 J g^{-1} [25].

2.6. Mechanical properties

The tensile properties of the composites were measured with an Instron TT-C-L tensile tester with a specially designed computerized data acquisition system at a stretching rate of 2.5 mm min^{-1}. The samples were produced with a ASTM Standard D 1708 die.

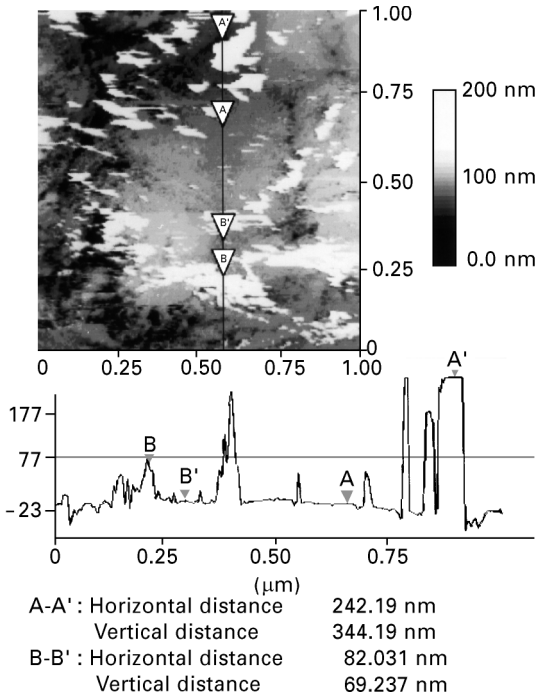

Figure 3 STM image of PPy-coated nickel flake (scan size, 1 μm × 1 μm; set point, 1 nA; bias voltage, 2 V).

3. Results and discussion

3.1. Particulate characterization

The weight fraction of PPy was determined to be approximately 5.8%. The large-scale structures of nickel and PPy-coated nickel flakes, observed under an optical microscope, were similar. Both were flakes of approximately 40 μm with sharp edges and the grain-boundary size of nickel and PPy-coated nickel were about the same (below 1 μm). No PPy particles were observed, indicating that the polymer was preferentially polymerized on the nickel surface.

STM was able to show the PPy coating on the surface of the nickel flakes. Fig. 3 is a 1 μm image of PPy-coated nickel. The grain boundaries were smaller than 1 μm and could also be observed with lateral force microscopy (not shown). Discrete aggregates of PPy protruding 300 nm or less from the surface were observed and were distorted by the probe owing to their polymeric nature. One possibility for depositing PPy aggregates on the surface is the rigorous stirring during the admicellar polymerization which may distort the film through collisions or abrasion of the flakes. As shown in the lower region of Fig. 3, surface protrusions, measured by section analysis, had a thickness ranging from 20 to 150 nm. The underlying PPy film is believed to be less than 10 nm, based on the lower limit of the thick parts. To understand the underlying PPy film further, a 0.5 cm × 0.5 cm nickel foil (0.1 mm; Alfa Aesar) was coated under the same conditions as the flake, except without stirring. Fig. 4 shows two images taken by AFM; the image on the left is bare nickel and the image on the right is PPy coated. The bare surface is granular in nature with a size of approximately 50 nm, whereas the size of the PPy-coated film is approximately 100 nm. This indicates that the PPy films grow in the form of the substrate structure and each particle in the right image may have enclosed several underlying substrate

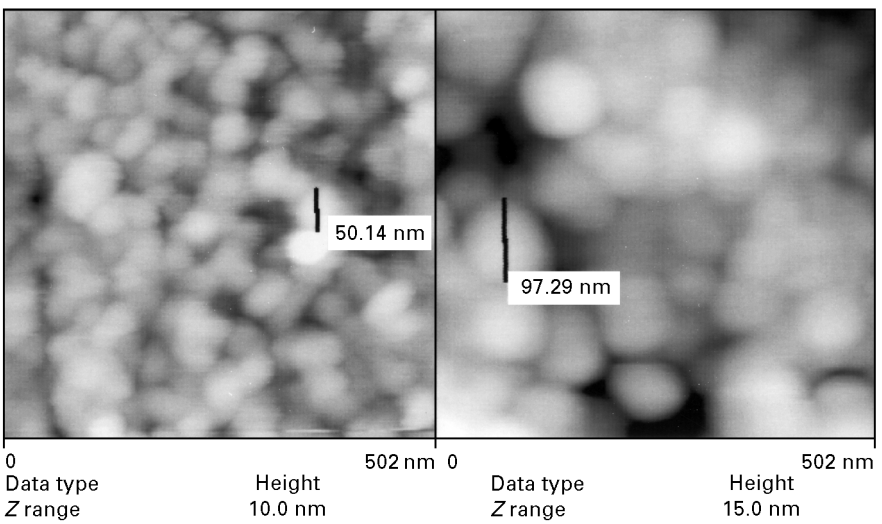

Figure 4 AFM images of bare (left) and PPy-coated (right) nickel foils (image size, 502 nm × 502 nm).

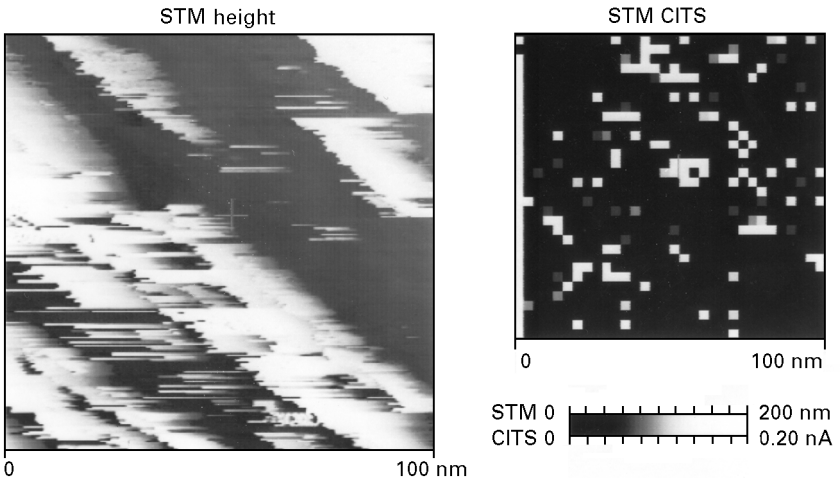

Figure 5 STM and CITS images of PPy-coated nickel (scan size, 100 nm × 100 nm; bias, 2 V; bias for CITS image, 1V).

grains. Since the height variation in both images is less than 10 nm, it is believed that the film thickness is also less than 10 nm. The underlying PPy film in the powder sample has not been resolved because a thickness of 10 nm falls within the target roughness range, 10–100 nm, of the nickel, which adds difficulty in distinguishing the film from the substrate in topographical images. Although the detailed morphology of PPy film was not obtained, the clusters continue to stay in position after successive STM scans and were enlarged for further investigation.

Fig. 5 is a 100 nm × 100 nm STM and CITS image of PPy-coated nickel at a 900 mV bias voltage. The left-hand image is a standard STM height image in which the tunnelling current is kept constant, while the image on the right is a CITS image. The figure shows that sites coated with PPy protrusions, as indicated by the bright regions, had lower tunnelling currents, whereas the brighter spots in CITS correspond to nickel surface with a PPy underlying thin film. Note also that the orientation of the PPy structure in the STM image is consistent with that of CITS and indicates that the resistivity of PPy is higher than that of nickel. The reported pure nickel resistivity is 6.97 μΩ cm while that of PPy is 2 mΩ cm [26, 27]. The resistivity shift indicates the presence of PPy patches on the surface of the nickel flakes.

The scanned image of the bare nickel sample shows no visible difference in surface morphology at a size from 100 nm to 1 μm. This means that the surface morphology prevails over that of the underlying polymer film. Individual and clustered strand-like structures have also been observed in the PPy-coated nickel images. No patchwise features resembling those of PPy-coated nickel were observed on bare nickel. In spite of the granular structure and a roughness from 10 to 20 nm, we can show through STM shows the existence of thickened patches of PPy on the nickel.

3.2. Conductivity

Fig. 6 shows the data from the conductivity testing for the nickel and PPy-coated nickel samples. The percolation thresholds for both the nickel and the PPy-coated nickel were approximately 5 vol%. Above the critical volume fraction the conductivity curves have the same shape, but there is an increase in conductivity of the PPy-coated nickel-filled LDPE composites by three orders of magnitude.

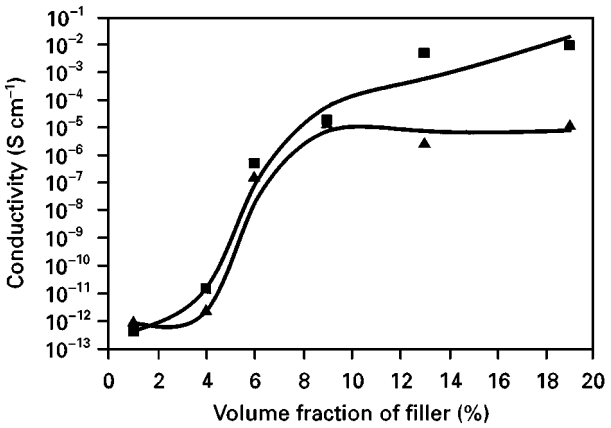

Figure 6 Conductivity versus concentration for nickel–LDPE (▲) and PPy-coated nickel–LDPE (■) composites. The curves are not fitted to theory and are only included to help to guide the eye.

Increased conductivity in the composite films at a given filler loading is a result of either a decrease in the resistivity of the filler, or a decrease in the particle–particle contact and/or tunnelling resistances. The resistivity of both the coated and the uncoated nickel flakes was measured as approximately 1.1 Ω cm. In order to determine whether the surface modification could have significantly increased the resistivity of the flakes, the resistivity with and without the addition of the PPy coating was calculated. For these simplified calculations, all resistances were assumed to be the same in each direction so that all the currents cancelled except for the current along the direction of the voltage drop. The randomly shaped flakes were modelled as uniform discs. The packing resistance, R_{pp}, of the powder was calculated using [12]

$$R_{pp} = \frac{\rho_f}{d} \quad (5)$$

where ρ_f ($= 6.97\,\mu\Omega\,cm$) is the intrinsic resistivity of the flakes and d is the contact diameter [2]. The average contact diameter was estimated to be approximately 0.79 μm via geometrical considerations. The approximate resistivity of the uncoated nickel flakes was calculated to be 2.8 Ω cm, which is close to the measured value of 1.1 Ω cm. Based on a uniform monolayer of the PPy coating the particle and the film resistance in series with the packing resistance, the estimated resistivity of the modified nickel powder was calculated to be approximately 8.8 Ω cm. While these values are only approximate, they show that the PPy coating could significantly increase the resistivity of the powder. This inconsistency between the measured and calculated trend in resistivity is probably due to non-uniform coating of the particles as observed in the STM images. Non-uniform coatings of PPy particulates have been reported in the literature using a different polymerization technique than the one used here [13]. Both the calculated and the experimental resistivities testing indicate that the increase in the conductivity of the composite is not a result of a lower filler resistance.

Since the conductivities of the nickel and PPy-coated powders are not significantly different, we believe the three-order-of-magnitude increase in conductivity is due to the combination of two phenomena. First, the admicellar coating reduces the particle–particle contact resistance. Fig. 7 is a schematic diagram of the possible interactions of the PPy coating with the polymer matrix. When the composite films are solution cast, PPy entanglements, acting as bridges, between the particles on adjacent filler particles are probably formed. These entanglements increase the contact area between the nickel particles by, in effect, becoming "molecular wires" connecting the filler particles, causing an increased contact area due to contacts of PPy particles outside the polymer matrix. As the PE matrix shrinks during solvent evaporation and crystallization, internal stresses place forces on the filler particles. This effect is enhanced by the PPy coating softening surface. The softer surface on the PPy-coated nickel particles will also increase the contact area. Second, entanglements between the PPy and the LDPE will "short circuit" the tunnelling resistance because the film thickness between the conductive pathways decreases owing to formation of conductive polymer paths between nickel particles.

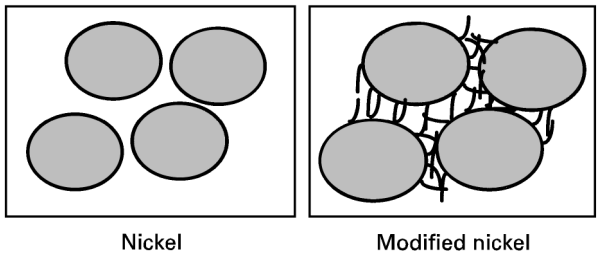

Figure 7 Schematic diagram of molecular wire formation in PPy-coated nickel–LDPE composites.

3.3. Crystallinity

As shown in Fig. 8, the crystallinity of LDPE increased with increasing volume fraction, indicating that both types of filler particle act as a nucleating agent for the materials. While the data indicate that the PPy coating does slightly increase the crystallinity at low volume fractions, there is no statistical difference in crystallinity at high filler loadings. The high branching of the LDPE matrix prevents the polymer from forming large crystalline regions and the crystallinity is consistent with other highly branched polyethylenes [28].

3.4. Mechanical properties

The tensile modulus of the composite materials increased with increasing volume fraction, as shown in Fig. 9. However, the elongation at break, shown in Fig. 10, and the ultimate strength, shown in Fig. 11, decreased exponentially by the initial addition of the nickel due to the creation of fracture points at the nickel–LDPE interface. The addition of the PPy coating to the nickel did not significantly change the mechanical properties as PPy is not miscible with LDPE. PPy is much stiffer than LDPE and is not soluble in xylene and may act as a mechanical reinforcing agent similar to nickel under these conditions. To test this hypothesis, the mechanical properties of a 29 vol% LDPE–PPy blend were measured. The blend showed

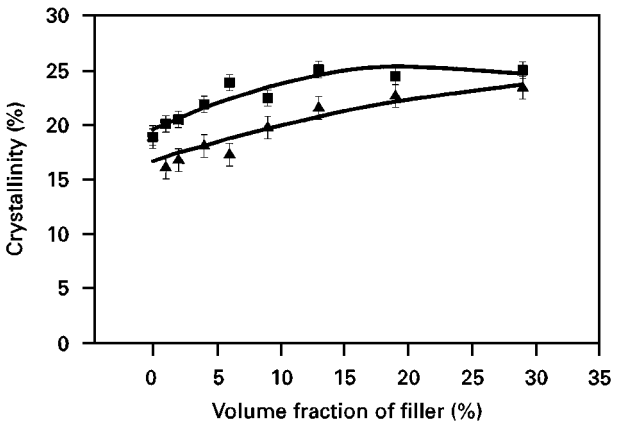

Figure 8 Crystallinity versus concentration of nickel–LDPE (▲) and PPy-coated nickel–LDPE (■) composites.

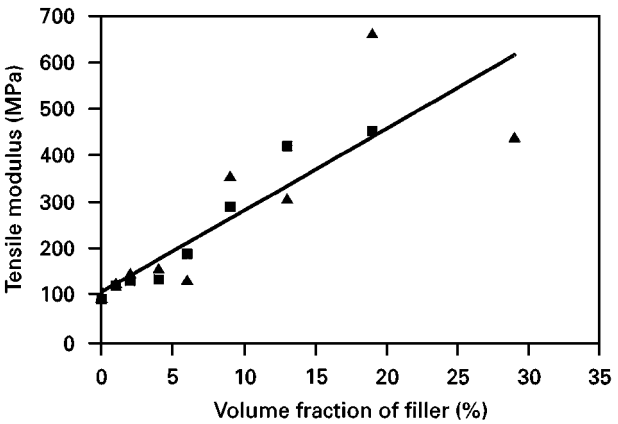

Figure 9 Tensile modulus versus concentration of nickel–LDPE (▲) and PPy-coated nickel–LDPE (■) composites.

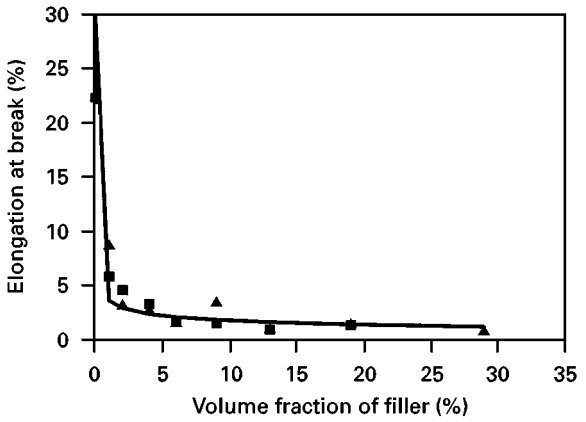

Figure 10 Elongation at break versus concentration of nickel–LDPE (▲) and PPy-coated nickel–LDPE (■) composites.

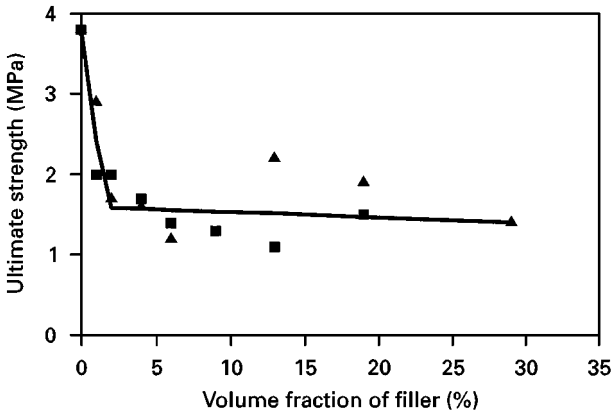

Figure 11 Ultimate strength versus concentration of nickel–LDPE (▲) and PPy-coated nickel–LDPE (■) composites.

similar values in tensile modulus, elongation at break, and ultimate strength as that of the metal-flake-filled composites. This indicates that the PPy is acting as a filler and that interfacial adhesion between the filler and the polymer matrix was not significantly changed by the addition of the PPy coating.

4. Conclusion

PPy coating via admicellar polymerization increases the conductivity of nickel-filled LDPE above the percolation threshold by approximately three orders of magnitude. This increase may be due to the formation of "molecular wires" created by PPy entanglements at the particle–particle interface. These entanglements probably decrease the particle–particle contact resistance by increasing the contact area of the filler particles and may also reduce the tunnelling resistance by decreasing the film thickness through which a conducting electron must hop.

The large-scale structures of PPy-coated nickel and nickel flakes are similar. The flake size is approximately 40 μm and no PPy particles mixed with PPy-coated nickel flakes were observed. The film-like and strand-like structures observed in STM images of PPy-coated nickel confirm the existence of PPy on the nickel flakes. The small-scale STM study showed that the film-like structure had a lower conductivity than the nickel substrate had.

The mechanical and thermal properties of the composite were not affected by the addition of the PPy coating. The crystallinity of the LDPE increases with increasing filler concentration. At higher volume fractions the coating did not statistically affect the crystallinity. The tensile modulus increased with increasing filler concentration, but the ultimate stress and elongation at break decreased with increasing filler concentration owing to poor polymer–filler adhesion. The mechanical properties of the composite were not affected by the addition of the PPy coating to the nickel particles as a result of the immiscibility of PPy in LDPE, thus not increasing adhesion at the polymer–filler interface.

Acknowledgement

Support for this project was provided by the National Science Foundation EPSCOR program (Cooperative Agreement OSR-9950478). Funding for the SPM system was provided by the Oklahoma Center for the Advancement of Science and Technology.

References

1. R. H. NORMAN, "Conductive rubbers and plastics" (Elsevier, New York, 1970) p. 3.
2. R. A. CROSSMAN, *Polym. Engng Sci.* **25** (1985) 507.
3. J. GURLAND, *Trans. Metall. Soc. AIME* **236** (1966) 642.
4. A. MALLIARIS and D. T. TURNER, *J. Appl. Phys.* **42** (1971) 614.
5. S. KIRKPATRICK, *Rev. Mod. Phys.* **45** (1973) 574.
6. S. M. AHARONI, *J. Appl. Phys.* **43** (1972) 2463.
7. F. LUX, *J. Mater. Sci.* **28** (1993) 285.
8. E. P. MAMUNYA, V. V. DAVIDENKO and E. V. LEBEDEV, *Polym. Compos.* **16** (1995) 319.
9. D. E. DAVENPORT, in "Polymer science and technology: conductive polymers", edited by R. B. Seymour (Plenum, New York, 1981) p. 39.
10. D. M. BIGG, *J. Rheol.* **25** (1984) 501.
11. T. YAMAMOTO, E. KUBOTA, A. TANIGUCHI, S. DEV, K. TANAKA and K. OSAKADA, *Chem. Mater.* **4** (1992) 570.
12. R. G. RUSCHAU, S. YOSHIKAWA and R. E. NEWNHAM, *J. Appl. Phys.* **72** (1992) 953.
13. S. P. ARMES, S. GOTTESFEILD, J. G. BEERY, F. GARZON and S. F. AGNEW, *Polymer* **32** (1991) 2325.
14. R. PARTCH, S. G. GANGOLLI, E. MATIJEVIC, W. CAI and S. ARAJS, *J. Colloid Interface Sci.* **144** (1991) 27.
15. G. P. FUNKHOUSER, M. P. AREVALO, D. T. GLATZHOFER and E. A. O'REAR, *Langmuir* **11** (1995) 1443.
16. M. A. FOX and K. L. WORTHEN, *Chem. Mater.* **3** (1991) 253.
17. M. GILL, S. P. ARMES, D. FAIRHURST, S. N. EMMETT, G. IDZOREK and T. PIGOTT, *Langmuir* **8** (1992) 2178.
18. C. L. HUANG, R. E. PARTCH and E. MATIJEVIC, *J. Colloid Interface Sci.* **170** (1995) 275.
19. E. P. PLUEDDEMANN, "Silane coupling agents" (Plenum, New York, 2nd Edn, 1991) pp. 206, 208.
20. J. H. O'HAVER, J. H. HARWELL, E. A. O'REAR, L. J. SNODGRASS and W. H. WADDELL, *Langmuir* **10** (1994) 2588.
21. G. P. FUNKHOUSER, M. P. AREVALO, D. T. GLATZHOFER and E. A. O'REAR, *ibid.* **11** (1995) 1443.
22. H. MORIWAKI, Y. YOSHIKAWA and T. MORIMOTO, *ibid.* **6** (1990) 847.
23. A. GUPTA, D. M. SIMPSON and I. R. HARRISON, *Plast. Engng* **49** (1993) 33.

24. E. M. BARRALL II and J. F. JOHNSON, in "Techniques and methods of polymer evaluation", Vol. 2, "Thermal characterization", edited by P. E. Slade and L. T. Jenkins (Marcell Dekker, New York, 1970) p. 2.
25. L. E. ALEXANDER, "X-ray diffraction methods in polymer science" (Robert E. Krieger Publishing, Malbar, FL, 1969) p. 478.
26. J. A. DEAN, "Lang's handbook of chemistry" (McGraw-Hill, New York, 14th Edn, 1992) p. 47.
27. J. R. FRIED, "Polymer science and technology" (Prentice-Hall, Englewood Cliffs, NJ, 1995) p. 463.
28. S. L. AGGARWAL, in "Polymer handbook", edited by J. Brandrup and E. M. Immergut (Wiley, New York, 2nd Edn, 1975) p. V-13.

Received 15 April 1997
and accepted 3 March 1998